Self-Assembly of Rings, Catenanes, and a Doubly Braided Catenane Containing Gold(I): The Hinge-Group Effect in Diacetylide Ligands

Christopher P. McArdle,[a] Michael C. Jennings,[a] Jagadese J. Vittal,[b] and Richard J. Puddephatt*[a]

Abstract: Reaction of the flexible dialkynyldigold(I) precursors $X(4\text{-}C_6H_4OCH_2CCAu)_2$ with 1,4-bis(diphenylphosphino)butane gave complexes of formula $[\{[\mu\text{-}X(4\text{-}C_6H_4OCH_2CCAu)_2][\mu\text{-}(Ph_2PCH_2CH_2CH_2CH_2PPh_2)]\}_n]$. The complexes exist as 25-membered ring compounds with $n=1$ when X = O or S, as [2]catenanes with $n=2$ when $X=CH_2$ or CMe_2, and as a unique doubly braided [2]catenane, containing interlocked 50-membered rings with $n=4$ when X = cyclohexylidene. These compounds form easily and selectively by self-assembly; reasons for the selectivity are also discussed.

Keywords: aurophilicity · catenanes · gold · molecular recognition · self-assembly

Introduction

The concept of molecular topology,[1] chemical isomerism arising from the consideration of non-Euclidean properties,[2] allows the systemization of interesting structures including catenanes, rotaxanes, and knots.[3–6] New synthetic strategies, based on ideas such as metal-ion templating[3] and self-assembly through non-covalent interactions,[4] have led to the realization of these original ideas through the synthesis of increasingly intricate molecular topologies.[5, 6] These supermolecules attract continued attention for their potential application in the development of nanoscale devices.[7]

A compound is said to be topologically nontrivial if it possesses nonplanar molecular graphs when embedded in three-dimensional space. In two-ring systems, mechanical bonds (nonbonded interconnections) can lead to the observation of simple molecular topology. Figure 1 depicts a pictorial representation of this concept, showing three possible arrangements of two "molecular" rings, each resulting in a different topological "isomer". While the simple rings (**A**) and [2]catenanes (**B**) are both well recognized at the molecular level, the doubly braided [2]catenane (**C**) has remained a serious synthetic challenge; it requires two rings to be interlocked not once but twice. The only successful reported approach to this problem has been to use multistep, metal-mediated reactions.[8] The syntheses are elegant and doubly braided [2]catenanes have been characterized by using NMR and MS techniques, though without the detailed structural information from an X-ray structure determination.

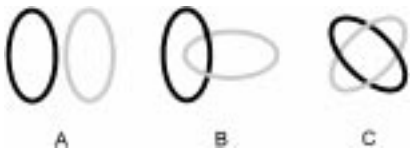

Figure 1. Schematic representation of topological stereoisomers.

There has been recent interest in the synthesis and characterization of new organometallic polymers with conjugated organic backbones leading towards potential applications as advanced materials.[9] If the polymers contain linear two-coordinate gold(I) centers,[10] there is the potential to orient the chains through aurophilic attractions between gold(I) atoms (shown as Au···Au, with typical distances of 2.75–3.40 Å and bond energies of 7–11 kcal mol^{-1}).[11] During this research, the first organometallic system that is predisposed for molecular recognition, leading to the self-assembly of interlocked molecular topographies, was discovered.[12] Reaction of flexible dialkynyl digold(I) complexes with diphosphine ligands can yield either simple ring or [2]catenane products in high yields. With a given diacetylide ligand, the outcome of the self-assembly reaction can depend on the number of methylene spacer groups n in the diphosphine ligand (Scheme 1).[12]

In this paper we describe how simple tailoring of the dialkynyl digold(I) complexes, in particular the "hinge" group X in alkynyl ligands derived from $X(4\text{-}C_6H_4OCH_2CCH)_2$, can

[a] Prof. R. J. Puddephatt, Dr. C. P. McArdle, Dr. M. C. Jennings
Department of Chemistry, University of Western Ontario
London, Ontario N6A 5B7 (Canada)
Fax: (1) 519-661-3022
E-mail: pudd@uwo.ca

[b] Prof. J. J. Vittal
Department of Chemistry, National University of Singapore
3 Science Drive, Singapore 117543 (Singapore)

0947-6539/01/0716-3572 $ 17.50+.50/0

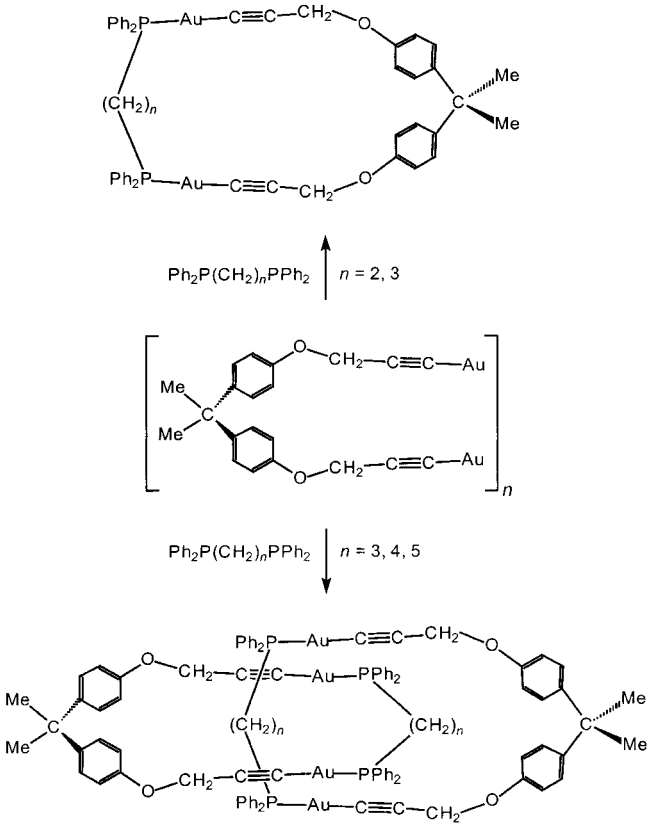

Scheme 1.

have a dramatic effect on the topology of the product macrocycles. The use of five different "hinge" groups resulted in the formation of three topologically distinct types of ring complex; two simple rings, two singly braided [2]catenanes, and one doubly braided [2]catenane. All five macrocycles have been fully characterized, and the basis for the self-assembly of the different structures is discussed. A preliminary report of some of these findings has been published.[13]

Results and Discussion

Ligand and gold(I) oligomer synthesis: Reaction of the bisphenol derivatives **1a–e** with propargyl bromide under basic conditions yields the bis(diethynyl)aryl ligands **2a–e** (Scheme 2), characterized by IR and NMR spectroscopy. Previous study in this research had focused on rigid (aryl) backbone diethynyl ligands, leading ultimately to polymeric type structures;[14] however, the new ligands possess a flexible tetrahedral hinge group (X = O, S, CH_2, CMe_2 or C_6H_{10} (cyclohexylidene)) that was expected to be conducive to the synthesis of ring complexes.

Diethynyls **2a–e** were converted into the oligomeric digold(I) diacetylide derivatives **3a–e** by reaction with [AuCl(SMe_2)] in the presence of sodium acetate (Scheme 2). Complexes **3a–e** were isolated, in almost quantitative yield, as yellow powders, which are insoluble in common organic solvents. Like other gold(I) acetylides, they are presumed to have a polymeric structure in which each acetylide is σ-bonded (η^1) to one gold atom and π-bonded (η^2) to another.[15] This is supported by IR spectroscopy, in which each of the oligomeric species **3a–e** exhibit a weak band at about 2000 cm^{-1}, considerably lower (ca. 120 cm^{-1}) than in the precursor diethynyl ligands **2a–e**, thus indicating that the alkynyl groups are acting as π donors. The insolubility of the oligomers did not allow characterization by solution NMR spectroscopy.

It is interesting to note that a rare example of an organometallic catenane was uncovered with the structural characterization of the "oligomeric" σ,π-type gold(I) acetylide, [(AuC≡C*t*Bu)$_6$].[16]

Synthesis of gold(I) macrocycles: Reaction of oligomers **3a–e** with bis(diphenylphosphino)butane (dppb) resulted in the formation of a series of soluble cyclic gold(I) complexes **4a–e**, as shown in Scheme 3. The new diphosphine complexes were isolated as air-stable white solids, and were characterized by elemental analysis, NMR (both one- and two-dimensional) and IR spectroscopy and X-ray structure determination. All reactions proceeded in an extremely facile manner and gave excellent yields (> 70 %). The new macrocyclic products are formed through a highly efficient self-assembly process. Remarkably, they exhibit three different types of molecular topology: the simple ring (**4a**,**b**), the singly braided [2]catenane (**4c**,**d**), and the doubly braided [2]catenane (**4e**).

In each reaction, elemental analysis was used to confirm the stoichiometry of phosphine addition. IR spectroscopy confirmed the presence of the acetylide groups in the products, with weak bands being observed in the spectra due to ν(C≡C), at approximately 2135 cm^{-1}. The ^{31}P NMR spectrum of each product exhibits one singlet at room temperature, an indication that there is only one species present and that the phosphine groups are effectively equivalent. The highly characteristic resonances (AA′XX′ multiplet) in the ^1H NMR spectra associated with the aryl (C_6H_4) groups of the digold backbones provided an excellent means for

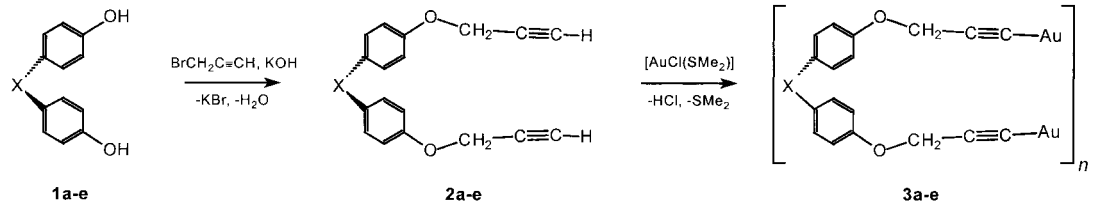

1a-e **2a-e** **3a-e**

a: X=O; **b**: X=S; **c**: X=CH_2; **d**: X=CMe_2; **e**: X=C_6H_{10}

Scheme 2.

  0947-6539/01/0716-3573 $ 17.50+.50/0

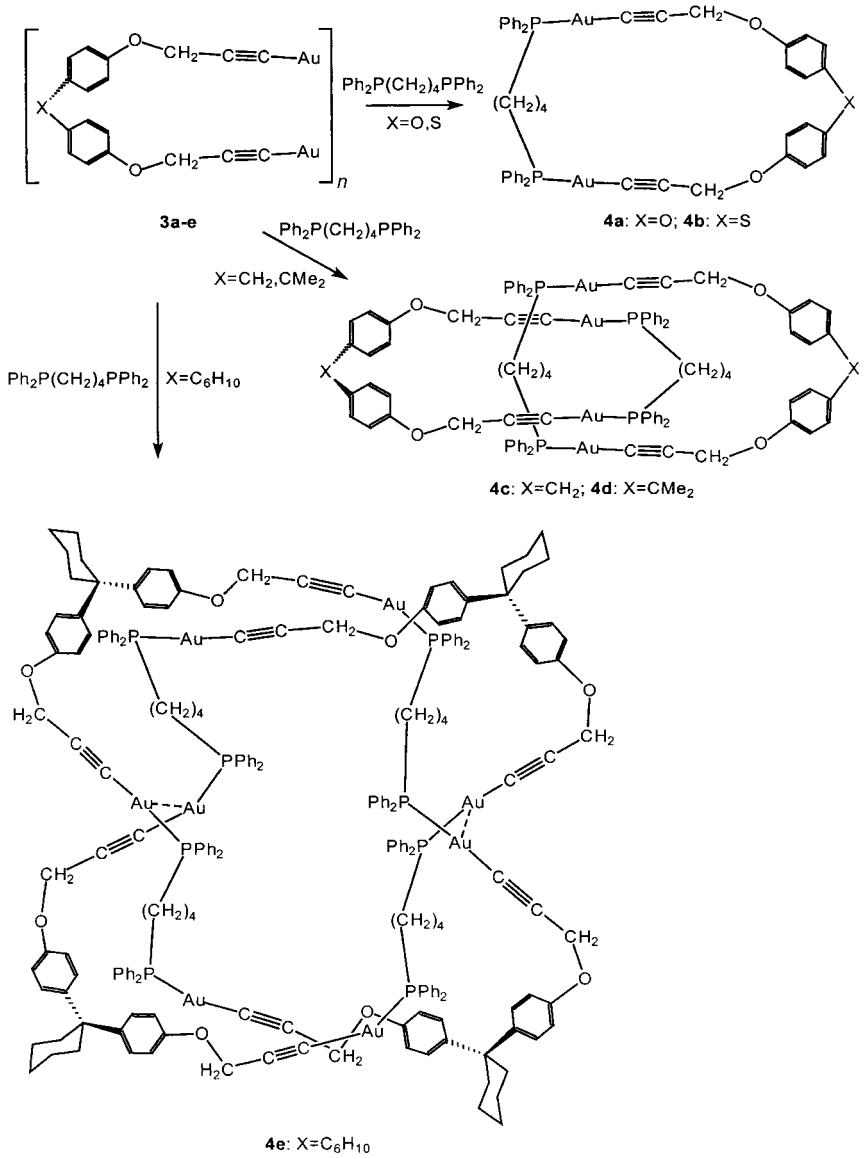

Scheme 3.

monitoring the progress of reactions and assessing the purity of the final products. The remaining protons of alkynyl and phosphine ligands gave the expected resonances, but could not be used to determine the topology of the products. ^{13}C NMR spectra were recorded and fully assigned for all the new products, and the details are listed in the Experimental Section. The data were consistent with a symmetrical arrangement of the macrocycles in solution. Both ethynyl carbon resonances appeared as doublets due to J(P,C) coupling (^2J(P-Au-C) ca. 140 Hz; ^3J(P-Au-C≡C) ca. 40 Hz).

^1H and ^{13}C two-dimensional NMR (COSY, gHSQC, gHMBC) techniques were used to demonstrate the connectivity within the product macrocycles, but they were unable to differentiate between the varying topological geometries. For the catenanes, NOESY and ROESY experiments did not show unusual cross-peaks due to close inter-ring contacts. In principle, mass spectrometry might give true molecular masses, but the techniques available (EI, CI, FAB, ESI) failed to give parent ions. Only X-ray structure determinations were successful in determining the topologies of **4a–e**. NMR studies of the recrystallized products then showed that the topological forms were maintained in solution.

Structural characterization: Discussion of the molecular structures will focus initially on the characteristics of the individual compounds. Table 1 provides a comparison of the important crystallographic features of the five structures.

*The simple ring complexes **4a** and **4b***: The molecular structure of simple ring **4a** (X = O), is shown in Figure 2, and selected bond lengths and angles are presented in Table 2. The ring is formed from the assembly of one diethynyldigold(I) unit and one diphosphine ligand, and so exists as a simple 25-membered ring. The ring can be considered to have an

Table 1. Comparison of structural data for compounds **4a–4e**.

	4a (X = O)	**4b** (X = S)	**4c** (X = CH_2)	**4d** (X = CMe_2)	**4e** (X = C_6H_{10})
macrocycle type	simple ring	simple ring	single braid [2]catenane	single braid [2]catenane	double braid [2]catenane
pseudoring shape	cyclopentane envelope	cyclopentane envelope	cyclopentane envelope	cyclopentane half-chair	cyclooctane twist-boat
d(Au···Au) intra [Å]	7.582	7.534	7.203, 7.068	7.809, 7.769	12.666, 12.452 12.842, 12.782
d(Au···Au) inter [Å]	9.361	10.279	3.585, 5.089	4.993, 5.219	3.239, 3.130 7.317, 7.858
hinge angle [°]	117.8(15)	104.3(3)	115.0(6) 115.3(5)	111.2(7) 111.9(9)	109(2), 110(2) 109(3), 106(2)
aryl twist [°]	1.6, 96.8	1.1, 97.2	33.1, 91.8 29.3, 92.6	46.9, 52.5 39.2, 49.4	74.2, 94.0 89.5, 105.9 108.8, 114.4 79.8, 84.4
aryl–aryl interactions[a]	2 ef	2 ef	2 off, 4 vf	2 off, 4 ef	12 ef

[a] ef: edge-to-face; vf: vertex-to-face; off: offset face-to-face.

0947-6539/01/0716-3574 $ 17.50+.50/0 *Chem. Eur. J.* **2001**, *7*, No. 16

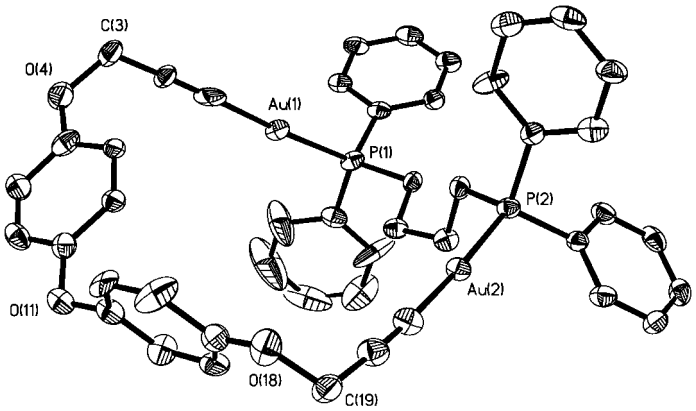

Figure 2. View of the structure of the simple ring complex **4a** (X = O).

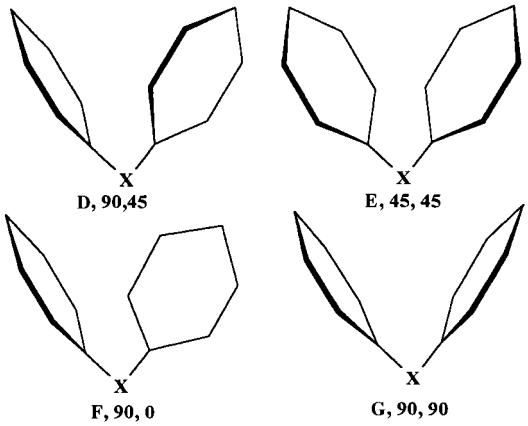

Figure 3. Conformations of the Ar_2X groups.

Table 2. Selected bond lengths [Å] and bond angles [°] for the simple ring **4a**.

Au(1)–P(1)	2.243(5)	Au(2)–P(2)	2.267(4)
Au(1)–C(1)	1.98(3)	Au(2)–C(21)	2.00(2)
C(1)–C(2)	1.20(3)	C(21)–C(20)	1.19(3)
C(2)–C(3)	1.43(3)	C(20)–C(19)	1.43(3)
C(3)–O(4)	1.44(3)	C(19)–O(18)	1.45(3)
O(4)–C(5)	1.39(2)	O(18)–C(17)	1.36(2)
C(10)–O(11)	1.38(2)	C(12)–O(11)	1.37(3)
C(22)-P(1)-Au(1)	113.2(6)	C(25)-P(2)-Au(2)	114.7(6)
P(1)-Au(1)-C(1)	176.6(6)	P(2)-Au(2)-C(21)	176.1(6)
Au(1)-C(1)-C(2)	176(2)	Au(2)-C(21)-C(20)	176(2)
C(1)-C(2)-C(3)	178(2)	C(21)-C(20)-C(19)	178(3)
C(2)-C(3)-O(4)	115(2)	C(20)-C(19)-O(18)	115(2)
C(3)-O(4)-C(5)	116(2)	C(19)-O(18)-C(17)	116(2)
C(10)-O(11)-C(12)	118(1)		

extended envelope structure, mapped by the atoms P(1)-P(2)-C(19)-O(11)-C(3), with C(3) at the "flap" vertex, and so it is evident that there is a large distortion from the most symmetrical possible structure that would have C_{2v} symmetry. The ring must be flexible, since the NMR data are consistent with C_{2v} symmetry. For example, equivalence of both the CH_2O and CH_2P protons is observed in the ^1H NMR spectrum of **4a**. There are no aurophilic interactions in the molecular or extended structure, and the bond lengths at the gold atoms (Au–P = 2.243(5) and 2.267(4) Å; Au–C = 1.98(3) and 2.00(2) Å) are normal for C≡C–Au–P coordination. The angle at the "hinge" oxygen atom, O(11), is C-O-C = 118(1)°. The two aryl (O-C_6H_4-O) rings adopt the so-called "Morino-structure" conformation (Figure 3 structure **F**),[17] one ring in the C-O-C plane and the other perpendicular (angle between the mean planes = 95.6°). This conformation is common in diaryl ethers and diaryl sulfides, probably to maximize π-bonding.[17] In the solid state, the rings form closely associated dimers (Figure 4a). This "dimer of simple rings" arises because the relative orientation of the aryl groups within each ring allows the perfect intermeshing in a manner that produces two close edge-to-face (ef) aryl–aryl attractive interactions:[18] each molecule provides an edge and a face, in a mutually beneficial arrangement. Phenyl–phenyl interactions have been shown to be weakly attractive (ca. 6 kJ mol^{-1}) forces, which often occur in clusters and so make a significant contribution to the formation and stability of particular structural motifs.[18] Further phenyl–phenyl offset-face-to face (off) interactions between adjacent dimeric pairs results in the formation of an extended array throughout the solid-state structure. The overall packing pattern of the "dimers" is very similar to the mixed herringbone and stacking pattern observed for many polycyclic aromatic compounds.

The molecular structure of the simple ring **4b** is shown in Figure 5, and the selected bond lengths and angles given in Table 3. The ring conformation and crystal packing is identical to that observed for the oxy-hinged simple ring. The pseudo cyclopentane envelope conformation is mapped by P(1)-C(3)-S(11)-C(19)-P(2), with C(3) at the "flap" vertex. The fold angle, 55°, is closely comparable with that found in **4a**, 57°, indicating that there is similar distortion from planarity in both the simple rings. The geometry at the sulfur atom, S(11), is comparable with that reported previously for diarylsulfide complexes, with angle the C-S-C = 104.3(3)° and C–S bond lengths of 1.772(5) and 1.759(5) Å.[19] The closest contact between any two gold atoms in the crystal structure is 7.534 Å (transannular Au···Au), so there are neither intra- nor intermolecular Au···Au attractions present in **4b**.

*The [2]catenanes **4c** and **4d***: The molecular structure of the singly braided [2]catenane **4c** is shown in Figure 6, and selected bond lengths and angles are summarized in Table 4. The catenane is formed by the self-assembly of two diethynyldigold(I) units and two diphosphine ligands to give two interlocking 25-membered rings. The individual components are similar to the simple rings **4a** and **4b**, adopting pseudo-cyclopentane-envelope conformations. In this case, however, there is less distortion from planarity with fold angles of 45° and 48°. The hinge angles C(10)-C(11)-C(12) = 115.0(6)° and C(40)-C(41)-C(42) = 115.3(5)° are also similar in the two rings.

There is a significant difference in the orientation of the C_6H_4 aryl groups in **4c** compared with **4a** and **4b**, as measured by the angles created between the planes of the aryl groups and the hinge plane (plane defined by the hinge atom and its two-bonded *ipso* carbon atoms). In the simple rings **4a** and **4b** the aryl groups are orientated such that one lies roughly parallel to the plane of the hinge unit, whilst the other is perpendicular. In **4c**, however, the aryl groups are positioned

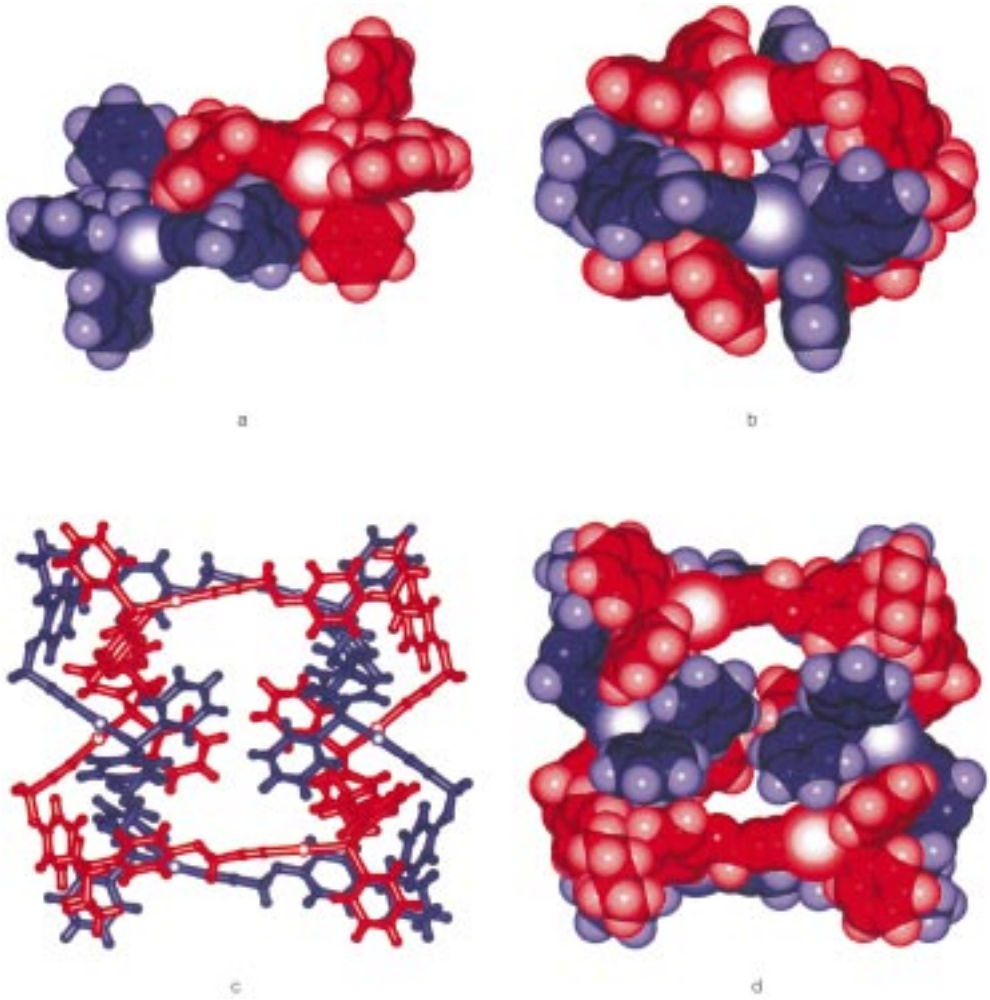

Figure 4. X-ray structure representations: a) a dimer pair of the simple ring complex **4a**, X = O (space-filling); b) the singly braided [2]catenane complex **4d**, X = CMe_2 (space-filling); c) the doubly braided [2]catenane complex **4e**, X = C_6H_{10} (ball and stick); d) the doubly braided [2]catenane complex **4e**, X = C_6H_{10} (space-filling).

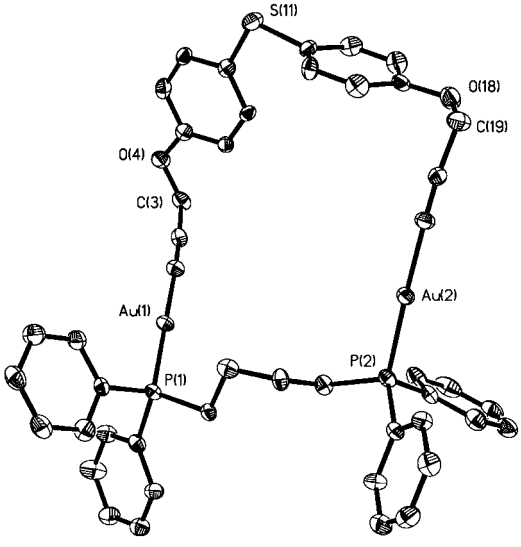

Figure 5. View of the structure of the simple ring complex **4b** (X = S).

Table 3. Selected bond lengths [Å] and bond angles [°] for the simple ring **4b**.

Au(1)–P(1)	2.271(2)	Au(2)–P(2)	2.272(2)
Au(1)–C(1)	2.00(1)	Au(2)–C(21)	2.006(9)
C(1)–C(2)	1.19(1)	C(21)–C(20)	1.17(1)
C(2)–C(3)	1.48(1)	C(20)–C(19)	1.48(1)
C(3)–O(4)	1.42(1)	C(19)–O(18)	1.43(1)
O(4)–C(5)	1.39(1)	O(18)–C(17)	1.38(1)
C(10)–S(11)	1.772(5)	C(12)–S(11)	1.759(5)
C(22)-P(1)-Au(1)	113.8(3)	C(25)-P(2)-Au(2)	113.2(3)
P(1)-Au(1)-C(1)	177.3(3)	P(2)-Au(2)-C(21)	174.3(3)
Au(1)-C(1)-C(2)	176.5(9)	Au(2)-C(21)-C(20)	176.3(9)
C(1)-C(2)-C(3)	177.3(9)	C(21)-C(20)-C(19)	174.3(10)
C(2)-C(3)-O(4)	113.2(8)	C(20)-C(19)-O(18)	111.4(7)
C(3)-O(4)-C(5)	117.9(6)	C(19)-O(18)-C(17)	118.6(7)
C(10)-S(11)-C(12)	104.3(3)		

with one perpendicular, and the other at about 30° to the plane of the hinge unit (between **D** and **E** in Figure 3). This apparently minor change in conformation is thought to influence the self-assembly to the catenane structure in **4c**.

The 25-membered rings in **4c** interlock across the methylene chain of the diphosphine ligand, and close examination of the catenane structure reveals extensive interaction between phenyl and aryl groups. In total, there are six attractive aryl–aryl interactions within the catenane, utilizing all the aromatic

0947-6539/01/0716-3576 $ 17.50+.50/0 *Chem. Eur. J.* **2001**, *7*, No. 16

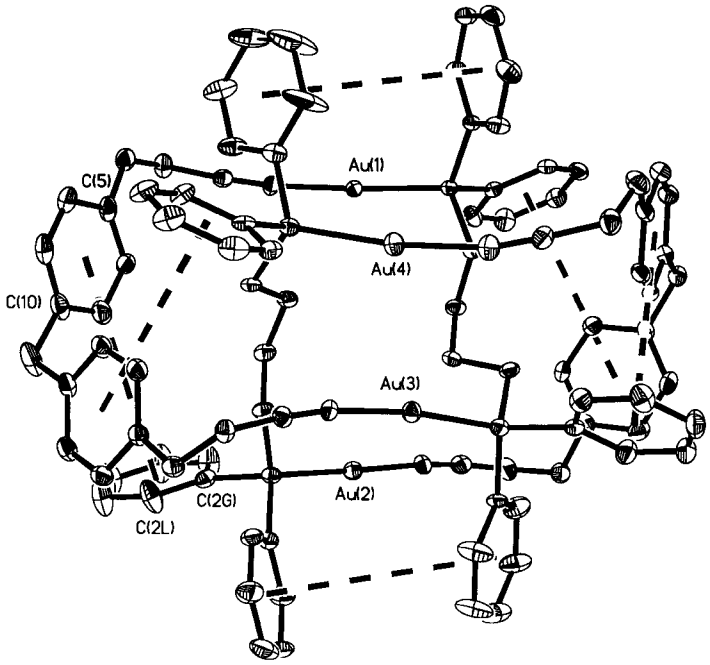

Figure 6. View of the structure of the singly braided [2]catenane complex **4c** (X = CH_2), showing aryl–aryl interactions (dotted lines).

Table 4. Selected bond lengths [Å] and bond angles [°] for the single braid [2]catenane **4c**.

Au(1)–P(1)	2.267(1)	Au(2)–P(2)	2.269(2)
Au(3)–P(3)	2.277(2)	Au(4)–P(4)	2.277(2)
Au(1)–C(1)	2.004(6)	Au(2)–C(31)	2.017(6)
Au(3)–C(21)	2.003(6)	Au(4)–C(51)	2.015(7)
C(1)–C(2)	1.177(8)	C(31)–C(32)	1.168(8)
C(21)–C(20)	1.171(8)	C(51)–C(50)	1.175(8)
C(2)–C(3)	1.481(9)	C(32)–C(33)	1.483(9)
C(20)–C(19)	1.499(8)	C(50)–C(49)	1.459(9)
C(3)–O(4)	1.425(7)	C(33)–O(34)	1.433(7)
C(19)–O(18)	1.411(7)	C(49)–O(48)	1.453(8)
O(4)–C(5)	1.370(9)	O(34)–C(35)	1.392(9)
O(18)–C(17)	1.366(7)	O(48)–C(47)	1.372(8)
C(10)–C(11)	1.481(11)	C(40)–C(41)	1.536(10)
C(11)–C(12)	1.541(9)	C(41)–C(42)	1.503(9)
C(22)-P(1)-Au(1)	113.0(2)	C(52)-P(2)-Au(2)	111.9(2)
C(25)-P(3)-Au(3)	112.8(2)	C(55)-P(4)-Au(4)	114.9(2)
P(1)-Au(1)-C(1)	176.5(2)	P(2)-Au(2)-C(31)	178.2(2)
P(3)-Au(3)-C(21)	172.5(2)	P(4)-Au(4)-C(51)	172.2(2)
Au(1)-C(1)-C(2)	173.8(7)	Au(2)-C(31)-C(32)	175.7(7)
Au(3)-C(21)-C(20)	170.7(6)	Au(4)-C(51)-C(50)	166.4(7)
C(1)-C(2)-C(3)	176.7(8)	C(31)-C(32)-C(33)	175.5(9)
C(21)-C(20)-C(19)	173.5(7)	C(51)-C(50)-C(49)	177.3(9)
C(2)-C(3)-O(4)	112.3(5)	C(32)-C(33)-O(34)	112.7(5)
C(20)-C(19)-O(18)	114.1(5)	C(50)-C(49)-O(48)	112.6(6)
C(3)-O(4)-C(5)	117.7(6)	C(33)-O(34)-C(35)	118.0(6)
C(19)-O(18)-C(17)	118.2(5)	C(49)-O(48)-C(47)	116.5(6)
C(10)-C(11)-C(12)	115.0(6)	C(40)-C(41)-C(42)	115.3(5)

rings within the molecule (two Ph···Ph off; four Ph···Ar vertex-to-face (vf)) as illustrated in Figure 6. The four vf interactions result from the aryl groups in the organogold backbone having the correct orientation for molecular recognition. The arrangement of the aryl groups in the complexes **4a** and **4b** is incorrect for this type of recognition. Clearly, the interlocking rings in **4c** give the maximum aryl–aryl interactions, and this appears to be sufficient to give an energetically favorable [2]catenane as product, overcoming the unfavorable entropy effect. Aryl-aryl interactions have previously been identified as playing an important role in the self-assembly of organic catenane complexes.[20] In complex **4c** the closest nonbonded Au···Au distances are 3.585 and 5.089 Å. The shorter distance is very close to the accepted range for aurophilic interactions (2.75–3.40 Å), and is probably weakly attractive.[11] Such gold···gold attractions could also favour catenane formation,[12] but closer approach of the gold atoms would lead to both steric repulsions and a weakening of the aryl–aryl attractions (notably the vf attraction between Ar[C(5)-C(10)] and Ph[C(2G)-C(2L)]). In **4c** it seems that the aryl–aryl attractions control the overall structure, but, in general, maximization of both aryl–aryl and gold···gold interactions can be expected when this is possible.

The molecular structure of the CMe_2-hinged, singly braided catenane **4d** is shown in Figure 7, and selected bond lengths and angles are presented in Table 5. The overall structure of **4d** is similar to, but more symmetrical than, the other singly braided catenane **4c**, with two crystallographically equivalent 25-membered rings interlocked symmetrically across the dppb methylene chains. The space-filling representation (Figure 4b) shows how the efficient braiding of the two rings produces a very compact structure, with pairwise matching of all the aromatic groups. The component rings in **4d** adopt

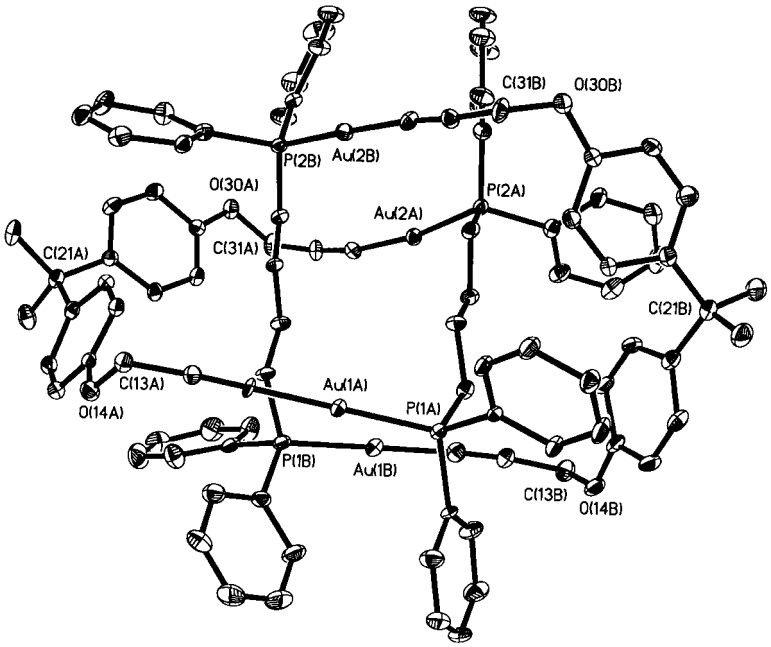

Figure 7. View of the structure of the singly braided [2]catenane complex **4d** (X = CMe_2).

Table 5. Selected bond lengths [Å] and bond angles [°] for the single braid [2]catenane **4d**.

Au(1A)–P(1A)	2.267(2)	Au(1B)–P(1B)	2.272(2)
Au(2A)–P(2A)	2.267(3)	Au(2B)–P(2B)	2.264(2)
Au(1A)–C(11A)	1.984(8)	Au(1B)–C(11B)	2.00(1)
Au(2A)–C(33A)	1.97(1)	Au(2B)–C(33B)	2.00(1)
C(11A)–C(12A)	1.22(1)	C(11B)–C(12B)	1.21(1)
C(33A)–C(32A)	1.21(1)	C(33B)–C(32B)	1.19(1)
C(12A)–C(13A)	1.45(1)	C(12B)–C(13B)	1.47(1)
C(32A)–C(31A)	1.48(1)	C(32B)–C(31B)	1.46(1)
C(13A)–O(14A)	1.45(1)	C(13B)–O(14B)	1.43(1)
C(31A)–O(30A)	1.45(1)	C(31B)–O(30B)	1.46(1)
O(14A)–C(15A)	1.35(1)	O(14B)–C(15B)	1.39(1)
O(30A)–C(29A)	1.36(1)	O(30B)–C(29B)	1.39(1)
C(20A)–C(21A)	1.56(1)	C(20B)–C(21B)	1.52(2)
C(21A)–C(24A)	1.54(1)	C(21B)–C(24B)	1.53(1)
C(1A)-P(1A)-Au(1A)	113.3(3)	C(1B)-P(1B)-Au(1B)	112.1(3)
C(4A)-P(2A)-Au(1A)	114.1(3)	C(4B)-P(2B)-Au(1B)	113.4(3)
P(1A)-Au(1A)-C(11A)	179.8(3)	P(1B)-Au(1B)-C(11B)	174.6(3)
P(2A)-Au(2A)-C(33A)	170.9(3)	P(2B)-Au(2B)-C(33B)	177.4(3)
Au(1A)-C(11A)-C(12A)	175.8(9)	Au(1B)-C(11B)-C(12B)	173.6(10)
Au(2A)-C(33A)-C(32A)	169.9(10)	Au(2B)-C(33B)-C(32B)	175.2(9)
C(11A)-C(12A)-C(13A)	177.7(11)	C(11B)-C(12B)-C(13B)	173.6(12)
C(33A)-C(32A)-C(31A)	174.3(12)	C(33B)-C(32B)-C(31B)	175.2(11)
C(12A)-C(13A)-O(14A)	112.4(8)	C(12B)-C(13B)-O(14B)	111.9(9)
C(32A)-C(31A)-O(30A)	113.2(8)	C(32B)-C(31B)-O(30B)	112.5(9)
C(13A)-O(14A)-C(15A)	119.1(8)	C(13B)-O(14B)-C(15B)	118.9(8)
C(31A)-O(30A)-C(29A)	115.5(8)	C(31B)-O(30B)-C(29B)	117.9(8)
C(20A)-C(21A)-C(24A)	111.2(7)	C(20B)-C(21B)-C(24B)	111.9(9)

extended cyclopentane half-chair conformations, mapped by [P(1A)-C(13A)-C(21A)-C(31A)-P(2A)] and [P(1B)-C(13B)-C(21B)-C(31B)-P(2B)]. The rings are twisted (fold angles of 33 (ring A)and 38 (ring B)°), with the two phosphorus atoms displaced on either side of the plane defined by the other atoms. There is less distortion of each ring from planarity in **4d** than in **4a–c**, which all adopt the extended envelope conformation.

The presence of methyl substituents on the hinge carbon atom [C(21A), C(21B)], does not greatly affect the hinge angle (C-C-C = 112(1)° in **4d** compared to 115° in **4c**), but it does cause a noticeable change in the orientation of the aryl (C_6H_4) groups. In **4d**, each aryl group is orientated at about 45° to the plane of the hinge (individual angles are 39 and 54°), such that the two aryl groups are mutually orthogonal (close to **E** in Figure 3). There are again six aryl–aryl attractions, but these are now comprised of four Ph···Ar ef and two Ph···Ph off attractions. The formation of ef attractions in **4d**, rather than vf interactions as seen in **4c**, is attributed to the different orientations of the aryl groups. There is no contribution from aurophilic attractions, since the shortest Au···Au distances (4.993(1) and 5.219(1) Å) are beyond the range for any bonding interaction. Importantly though, the molecular recognition for the successful interlocking of the two rings is still present, and the total number of attractive forces is maintained. Hence, the necessary energy to drive the self-assembly process is available.

*The doubly braided catenane **4e***: The structure determination of the doubly braided [2]catenane **4e** is the first for such compounds, which have been identified previously by using NMR and MS techniques.[8] The molecular structure of one enantiomer of **4e** (doubly braided catenanes are inherently chiral) is shown in Figure 8, and selected bond lengths and angles are listed in Table 6.

The product results from the remarkable self-assembly of eight components (four organogold units and four dppb ligands) and consists of two giant 50-membered rings doubly braided in a highly effective manner. The efficiency and selectivity of this complex reaction is particularly impressive, and provides a beautiful example of the power of molecular recognition. The space-filling diagram, Figure 4d, provides an excellent illustration of the complex intertwining and the compact nature of the catenane structure (two solvent dichloromethane molecules that are not shown, pack the remaining cavity space).

The component 50-membered rings each consist of two organogold backbones linked, in a linear fashion, by two dppb ligands creating a large "double ring". Both adopt extended cyclooctane twist-boat conformations, mapped by the atom groupings [C(34)-C(46)-P(3)-P(4)-C(10)-C(3)-P(1)-P(2)] and [C(58)-C(51)-P(7)-P(8)-C(82)-C(75)-P(5)-P(6)], respectively, with the twists centered about the P–P vertices. The twist-boat form is uncommon in cyclooctane, owing to severe eclipsing strain, but in these large organometallic rings (Au···Au transannular distances ca. 12–13 Å) this problem is not a factor. Overall, though, this conformation does cause the rings

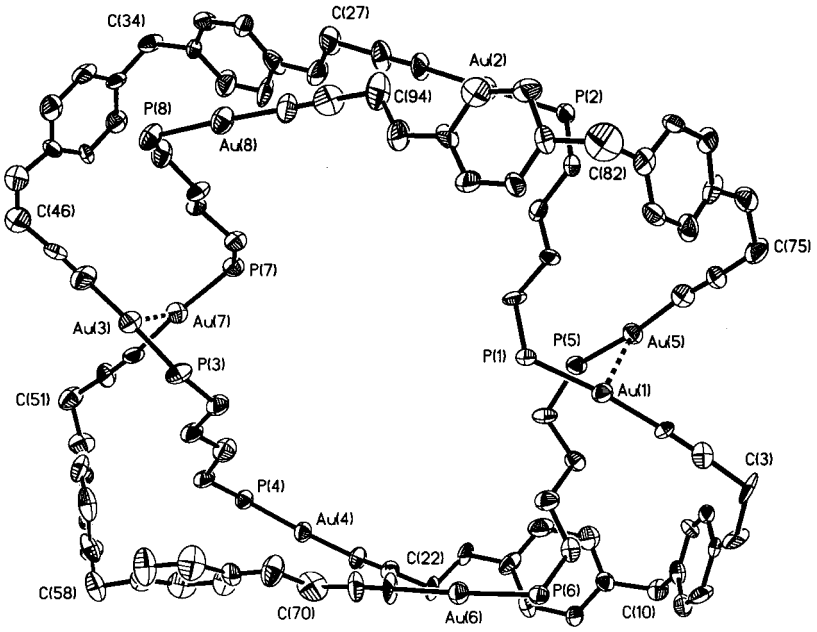

Figure 8. View of the structure of the doubly braided [2]catenane complex **4e** (X = C_6H_{10}) showing core ring atoms only (phenyl rings of the diphosphine ligands and cyclohexylidene groups are omitted for clarity).

0947-6539/01/0716-3578 $ 17.50+.50/0 *Chem. Eur. J.* **2001**, *7*, No. 16

Table 6. Selected bond lengths [Å] and bond angles [°] for the double braid [2]catenane **4e**.

Au(1)–Au(5)	3.239(2)	Au(7)–Au(3)	3.130(2)
Au(1)–P(1)	2.283(7)	Au(5)–P(5)	2.279(7)
Au(2)–P(2)	2.286(7)	Au(6)–P(6)	2.279(7)
Au(3)–P(3)	2.284(9)	Au(7)–P(7)	2.285(8)
Au(4)–P(4)	2.291(7)	Au(8)–P(8)	2.271(8)
Au(1)–C(1)	1.95(2)	Au(5)–C(73)	2.00(3)
Au(2)–C(25)	1.98(3)	Au(6)–C(72)	2.04(3)
Au(3)–C(48)	1.98(4)	Au(7)–C(49)	2.02(3)
Au(4)–C(24)	2.02(3)	Au(8)–C(96)	1.97(3)
C(1)–C(2)	1.25(3)	C(73)–C(74)	1.18(3)
C(25)–C(26)	1.17(4)	C(71)–C(72)	1.07(3)
C(48)–C(47)	1.18(4)	C(49)–C(50)	1.17(4)
C(24)–C(23)	1.14(3)	C(95)–C(96)	1.24(4)
C(7)–C(10)	1.55(4)	C(55)–C(58)	1.53(5)
C(10)–C(16)	1.56(4)	C(58)–C(64)	1.54(4)
C(31)–C(34)	1.53(3)	C(79)–C(82)	1.63(4)
C(34)–C(40)	1.54(4)	C(82)–C(88)	1.62(4)
C(1)-Au(1)-P(1)	174.1(8)	C(73)-Au(5)-P(5)	171.9(9)
C(25)-Au(2)-P(2)	178(1)	C(72)-Au(6)-P(6)	175(1)
C(48)-Au(3)-P(3)	171(1)	C(49)-Au(7)-P(7)	171.7(9)
C(24)-Au(4)-P(4)	177.1(9)	C(96)-Au(8)-P(8)	178(1)
C(2)-C(1)-Au(1)	177(2)	C(74)-C(73)-Au(5)	173(3)
C(26)-C(25)-Au(2)	176(4)	C(71)-C(72)-Au(6)	177(4)
C(47)-C(48)-Au(3)	178(4)	C(50)-C(49)-Au(7)	172(3)
C(23)-C(24)-Au(4)	176(3)	C(95)-C(96)-Au(8)	178(3)
C(7)-C(10)-C(16)	109(2)	C(55)-C(58)-C(64)	109(3)
C(31)-C(34)-C(40)	110(2)	C(79)-C(82)-C(88)	106(2)

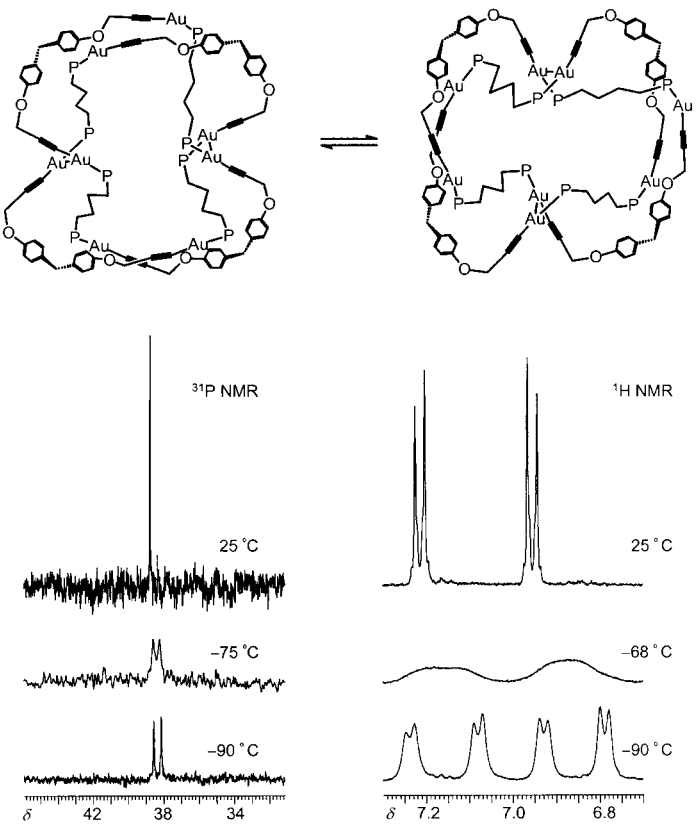

Figure 9. Variable temperature NMR observations of complex **4e**, and the proposed molecular switching motion.

to be heavily distorted from planarity, a necessary requirement to allow double, but not single, braiding.

Despite the formation of a different ring type, which now contains two hinge units, the geometry at the gold atoms and hinge carbon atoms, C(10), C(34), C(58) and C(82), is closely comparable with that seen in the simple rings and singly braided [2]catenanes, with no unusual bond lengths or angles (see Table 6). However, examination of the complete diaryl backbone reveals, once again, an important difference in the aryl group orientations. The aryls in the double rings are now all oriented nearly perpendicular to the plane of the hinge unit, with an average angle of approximately 80° (close to **G** in Figure 3). This small change, through its effect on the pre-organization for aryl–aryl interactions, has dramatically altered the molecular recognition of the system.

The complete structure contains, in total, 14 attractive interactions: two Au···Au, four Ph–Ph ef, and eight Ar–Ph ef; these are evidently sufficient to drive the catenation. The phenyl–aryl interactions occur at the outer corners of the tightly packed structure, whilst the phenyl–phenyl interactions are situated within the center of the catenane. The short attractive aurophilic attractions (Au(1)···Au(5) 3.2387(16) and Au(3)····Au(7) 3.1296 Å) provide additional inter-ring secondary bonding. Figure 8 shows that the geometrical constraints imposed by double braiding do not allow all gold atoms to be close enough for Au···Au bonding. Thus the pairs of gold atoms Au(1)/Au(5) and Au(3)/Au(7) are close, but Au(2)/Au(8) and Au(4)/Au(6) are too far apart for Au···Au bonding.

Variable temperature NMR studies: The ^{1}H and ^{31}P NMR spectra of the simple ring complexes **4a** and **4b** and the singly braided [2]catenanes **4c** and **4d** are essentially unchanged over the temperature range −80 °C to 20 °C. For example, each gives only one singlet resonance in the ^{31}P NMR spectrum. This indicates that the rings are sufficiently flexible to give effective C_{2v} symmetry in each case. A number previous reports on singly braided [2]catenanes have demonstrated the existence of both intramolecular spinning and rotating processes.[22] For the [2]catenanes **4c** and **4d**, extensive snaking of the rings will be impossible because of steric effects of the bulky diphenylphosphino groups, but more limited rocking and wagging motions are possible and can lead to the effective equivalence of all phosphorus atoms. Such motions will lead to making and breaking of many of the secondary aryl–aryl bonding forces.

The variable temperature NMR studies of the doubly braided catenane **4e**, however, provide important information about the solution structure. One significant aspect of the solid-state structure, which is a consequence of the aurophilic interactions, is that for all the ring atoms (except the hinge atom) there are two chemically distinct environments. These are atoms that are closer to or further from the gold atoms which are engaged in close inter-ring aurophilic attractions. The overall symmetry is then close to C_2. However, the room temperature NMR data for **4e** indicates effective D_4 symmetry (the ideal symmetry for a doubly braided catenane as in Figure 1 **C**) and so suggests that the doubly braided [2]catenane is fluxional or that it exists in a different form in solution.

The room temperature ^{31}P NMR of **4e** has only one resonance, but as the sample is cooled down the signal resolves until at −90 °C the spectrum contains two resonances

(see Figure 9), as expected for the C_2 structure of Figure 8. Clearly the catenane is fluxional at room temperature. The activation energy at the coalescence temperature of $-70\,^{\circ}C$ was $\Delta G^{\ddagger} = 41(\pm 1)$ kJ mol^{-1}.

The variable temperature ^{1}H NMR data revealed, as expected, similar coalescence of inequivalent resonances. However, due to solvent limitations it was only possible to observe full resolution of one set of signals, the aryl (C_6H_4) group resonances (Figure 9). At room temperature a single AA′XX′ signal is observed, whilst at $-90\,^{\circ}C$ two AA′XX′ signals are clearly seen. The coalescence temperature was found to be $-68\,^{\circ}C$, giving an activation energy of $\Delta G^{\ddagger} = 41(\pm 1)$ kJ mol^{-1}, which shows good correlation with that calculated from the ^{31}P NMR spectra.

Fluxional behavior has previously been reported for a doubly braided catenane in solution.[22] It was preposed that the interlocked rings were undergoing slow gliding motions, analogous to the reptation process seen for a trefoil knot.[22] In complex **4e**, however, extensive snaking of the two rings would be impossible, as it would require the eclipsing of bulky diphenylphosphino substituents. The least motion that can cause the equivalence observed for **4e** would be a rapid back-and-forth switching action, indicated schematically in Figure 9. This dynamic motion requires making and breaking of Au···Au and aryl–aryl secondary bonds, but should not encounter strong steric hindrance. It is clear that any fluxionality observed for doubly braided catenanes will need to be determined on an individual basis, and could involve either extensive ring snaking or, as in **4e**, more limited molecular switching.

Conclusion

This work has shown that the reaction of flexible dialkynyldigold(I) compounds $X(C_6H_4OCH_2CCAu)_2$ with bis(diphenylphosphino)butane can lead to simple rings, [2]catenanes, or to a unique doubly braided [2]catenane depending on the nature of the hinge group X. The products are formed by simple self-assembly, and it is interesting to attempt to determine what properties of the group X are important in controlling the nature of the self-assembly process. The reactions are very selective in all cases, giving rise to a single isomeric form, though it is known that other diphosphine ligands can give isomeric mixtures.[12] Since the gold(I) centers are labile, the structures are not rigidly locked and could rearrange; the structures are determined by thermodynamic rather than kinetic control.[12] In principle, the C-X-C angle could be an important factor, since opening or closing of this angle would affect the size and shape of an individual ring cavity. However, the angles are not markedly different (Table 1) and no such correlation could be made. The chief differences observed were in the conformations adopted by the $X(C_6H_4\cdot)_2$ groups (Figure 3). There is naturally some question about whether this conformation determines the overall structure or vice versa, but there is some evidence as outlined below.

The Cambridge Structural Database (CSD) contains many X-ray structures that contain the same parent bisphenol units as those discussed here.[21] Examination of these structures revealed that the orientation of the aryl groups is, in most cases, very similar to that found in the corresponding organogold macrocycles **4a**–**e**. This correlation of the orientations of aryl groups in precursors and products suggests that it is, at least in part, the aryl orientation that determines the preferred mode of self-assembly. In particular, conformation **F** in Figure 3, found in **4a** and **4b** when X = O or S, appears to prevent catenation, presumably because the in-plane aryl group causes steric hindrance. Conformation **G** allows maximum catenation and is observed for the doubly braided catenane **4e**. Intermediate conformations such as **D** or **E**, found in **4c** and **4d**, allow singly braided [2]catenane formation. This empirical correlation, if confirmed by further examples, can be used in predicting the products of reaction of other derivatives $X(C_6H_4OCH_2CCAu)_2$ with diphosphines, by considering the orientation of the aryl groups in the parent bis(phenol). It is clear from this work that subtle effects at the hinge group have dramatic consequences on the self-assembly.

Experimental Section

NMR spectra were recorded using Varian Gemini 300, Mercury 400, and Inova 600 MHz spectrometers. ^{1}H and ^{13}C NMR chemical shifts are reported relative to tetramethylsilane, while ^{31}P chemical shifts are reported relative to 85% H_3PO_4 as an external standard. IR spectra were recorded using a Perkin–Elmer 2000 FTIR as Nujol mulls on KBr plates or as CH_2Cl_2 solutions in 0.1 mm NaCl cell. All gold complexes were protected from light by using darkened reaction flasks. The complex [AuCl(SMe$_2$)] was prepared by the literature method.[24]

Diacetylide ligand 2a: $BrCH_2C{\equiv}CH$ (7.06 g, 59.3 mmol) and finely ground KOH (3.50 g, 62.4 mmol) was added to a solution of $O(4\text{-}C_6H_4OH)_2$ (4.00 g, 19.8 mmol) in acetone (50 mL). The mixture was heated under reflux for about 16 h. The solution was allowed too cool to room temperature and then filtered to give a pale yellow filtrate. The solvent was removed under reduced pressure, and the resultant pale yellow oil dried under vacuum (3 days). The product was washed with pentane and dried further. Yield: 4.75 g, 86%; IR (Nujol): $\tilde{\nu} = 2048$ (br, w), 2121 cm^{-1} (s) (C≡C); ^{1}H NMR (300 MHz, CD_2Cl_2, 25 °C): $\delta = 6.94$ (m, 4H; C_6H_4), 4.68 (d, $J = 2.4$ Hz, 4H; OCH_2), 2.59 (t, $J = 2.4$ Hz, 2H; C≡CH); ^{13}C NMR (75 MHz, CD_2Cl_2, 25 °C): $\delta = 153.7$, 152.4, 119.9, 116.4 (all C_6H_4), 79.1 (*C*≡CH), 75.6 (C≡*C*H), 56.7 (OCH_2); MS: *m*/*z* (%): 278 (67) $[M]^+$.

Diacetylide ligand 2b: This was prepared by the procedure described for **2a**, but with $S(4\text{-}C_6H_4OH)_2$ (4.00 g, 18.3 mmol), $BrCH_2C{\equiv}CH$ (6.54 g, 55.0 mmol), and KOH (3.20 g, 57.0 mmol). The product was isolated as a dark orange oil. Yield: 4.87 g, 90%; IR (Nujol): $\tilde{\nu} = 2013$ (br, w), 2122 cm^{-1} (s) (C≡C); ^{1}H NMR (300 MHz, CD_2Cl_2, 25 °C): $\delta = 7.29$ (m, 4H; C_6H_4), 6.92 (m, 4H; C_6H_4), 4.68 (d, $J = 2.4$ Hz, 4H; OCH_2), 2.14 (t, $J = 2.4$ Hz, 2H; C≡CH); ^{13}C NMR (75 MHz, CD_2Cl_2, 25 °C): $\delta = 157.4$, 133.1, 128.7, 116.0 (all C_6H_4), 78.7 (*C*≡CH), 75.8 (C≡*C*H), 56.3 (OCH_2); MS: *m*/*z* (%): 294 (76) $[M]^+$.

Diacetylide ligand 2c: This was prepared by the procedure described for **2a**, but with $H_2C(4\text{-}C_6H_4OH)_2$ (0.250 g, 1.25 mmol), $BrCH_2C{\equiv}CH$ (0.557 g, 3.74 mmol), and KOH (0.220 g, 3.90 mmol). The product was isolated as a pale yellow oil. Yield: 0.305 g, 88%; IR (Nujol): $\tilde{\nu} = 2047$ (w), 2121 cm^{-1} (m) (C≡C); ^{1}H NMR (400 MHz, CD_2Cl_2, 25 °C): $\delta = 7.11$ (m, 4H; C_6H_4), 6.88 (m, 4H; C_6H_4), 4.66 (d, $J = 2.4$ Hz, 4H; OCH_2), 3.87 (s, 2H; CH_2), 2.55 (t, $J = 2.4$ Hz, 2H; C≡CH); ^{13}C NMR (100 MHz, CD_2Cl_2, 25 °C): $\delta = 156.2$, 135.1, 130.0, 115.1 (all C_6H_4), 79.1 (*C*≡CH), 75.4 (C≡*C*H), 56.1 (OCH_2), 40.4 (CH_2); MS: *m*/*z* (%): 276 (100) $[M]^+$.

Diacetylide ligand 2d: This was prepared by the procedure described for **2a**, but with $Me_2C(4\text{-}C_6H_4OH)_2$ (10.0 g, 43.8 mmol), $BrCH_2C{\equiv}CH$ (15.6 g, 131.4 mmol), and KOH (7.6 g, 135.4 mmol). The product was isolated as a pale yellow solid. Yield: 10.7 g, 80%; IR (Nujol): $\tilde{\nu} = 2028$ (w), 2120 cm^{-1} (m) (C≡C); ^{1}H NMR (300 MHz, CD_2Cl_2, 25 °C): $\delta = 7.17$ (m, 4H; C_6H_4), 6.88 (m, 4H; C_6H_4), 4.67 (d, $J = 2.4$ Hz, 4H; OCH_2), 2.53 (t, $J = 2.4$ Hz, 2H; C≡CH), 1.65 (s, 6H; Me); ^{13}C NMR (75 MHz, CD_2Cl_2, 25 °C): $\delta = 155.8$,

0947-6539/01/0716-3580 $ 17.50+.50/0 *Chem. Eur. J.* **2001**, *7*, No. 16

144.3, 128.1, 114.5 (all C_6H_4), 79.2 (*C*≡CH), 75.5 (C≡*C*H), 56.1 (OCH_2), 42.0 (*C*Me_2), 31.0 (Me); MS: *m*/*z* (%): 304 (28) $[M]^+$.

Diacetylide ligand 2e: This was prepared by the procedure described for **2a**, but with $H_{10}C_6(4\text{-}C_6H_4OH)_2$ (4.0 g, 14.9 mmol), $BrCH_2C{\equiv}CH$ (5.32 g, 44.7 mmol), and KOH (2.60 g, 46.3 mmol). The product was isolated as a bright orange oil. Yield: 4.38 g, 85%; IR (Nujol): $\tilde{\nu}$ = 2049 (br, w), 2121 cm^{-1} (s) (C≡C); ^1H NMR (300 MHz, CD_2Cl_2, 25 °C): δ = 7.21 (m, 4H; C_6H_4), 6.88 (m, 4H; C_6H_4), 4.66 (d, J = 2.4 Hz, 4H; OCH_2), 2.56 (t, J = 2.4 Hz, 2H; C≡CH), 2.24 (m, 4H; C_6H_{10}), 1.51 (m, 6H; C_6H_{10}); ^{13}C NMR (75 MHz, CD_2Cl_2, 25 °C): δ = 155.5, 142.3, 128.3, 114.7 (all C_6H_4), 79.2 (*C*≡CH), 75.4 (C≡*C*H), 56.1 (OCH_2), 45.3, 37.5, 31.9, 29.4, 26.7, 23.3 (all C_6H_{10}); MS: *m*/*z* (%): 344 (29) $[M]^+$.

Caution: Some gold acetylides are potentially explosive; they should be prepared in small quantities and not subjected to shock!

Digold(I) diacetylide 3a: $[AuCl(SMe_2)]$ (0.400 g, 1.36 mmol) was dissolved in THF (100 mL)/MeOH (50 mL). A solution of **2a** (0.189 g, 0.68 mmol) and NaO_2CMe (0.167 g, 2.04 mmol) in THF (20 mL)/MeOH (20 mL) was added to this. The resulting mixture was stirred for 8 h to produce a bright yellow precipitate. The solid was then collected by filtration, washed with THF, MeOH, Et_2O and pentane, and dried. Yield: 0.326 g, 72%. The product was insoluble in common organic solvents. IR (Nujol): $\tilde{\nu}$ = 1999 cm^{-1} (w) (C≡C); elemental analysis calcd (%) for $C_{18}H_{12}Au_2O_3$ (670.2): C 32.26, H 1.80; found: C 32.55, H 1.88.

Digold(I) diacetylide 3b: This was prepared by the procedure described for **3a** from $[AuCl(SMe_2)]$ (0.400 g, 1.36 mmol), **2b** (0.200 g, 0.68 mmol), and NaO_2CMe (0.167 g, 2.04 mmol). The product was isolated as an insoluble yellow solid. Yield: 0.343 g, 74%; IR (Nujol): $\tilde{\nu}$ = 2002 cm^{-1} (w) (C≡C); elemental analysis calcd (%) for $C_{18}H_{12}Au_2O_2S_1$ (686.3): C 31.50, H 1.76; found: C 30.89, H 1.95.

Digold(I) diacetylide 3c: This was prepared by the procedure described for **3a** from $[AuCl(SMe_2)]$ (0.650 g, 2.21 mmol), **2c** (0.305 g, 1.10 mmol), and NaO_2CMe (0.272 g, 3.31 mmol). The product was isolated as an insoluble yellow solid. Yield: 0.678 g, 92%; IR (Nujol): $\tilde{\nu}$ = 2003 cm^{-1} (w) (C≡C); elemental analysis calcd (%) for $C_{19}H_{14}Au_2O_2$ (668.3): C 34.15, H 2.11; found: C 34.49, H 2.13.

Digold(I) diacetylide 3d: This was prepared by the procedure described for **3a** from $[AuCl(SMe_2)]$ (0.593 g, 2.01 mmol), **2d** (0.306 g, 1.01 mmol), and NaO_2CMe (0.412 g, 5.02 mmol). The product was isolated as an insoluble yellow solid. Yield: 0.661 g, 94%; IR (Nujol): $\tilde{\nu}$ = 2000 cm^{-1} (w) (C≡C); elemental analysis calcd (%) for $C_{21}H_{18}Au_2O_2$ (696.3): C 36.22, H 2.61; found: C 35.93, H 2.45.

Digold(I) diacetylide 3e: This was prepared by the procedure described for **3a** from $[AuCl(SMe_2)]$ (0.400 g, 1.36 mmol), **2e** (0.234 g, 0.68 mmol), and NaO_2CMe (0.167 g, 2.04 mmol). The product was isolated as an insoluble yellow solid. Yield: 0.417 g, 83%; IR (Nujol): $\tilde{\nu}$ = 2003 (w) cm^{-1} (C≡C); elemental analysis calcd (%) for $C_{24}H_{22}Au_2O_2$ (736.4): C 39.15, H 3.01; found: C 39.57, H 2.82.

Simple ring 4a: A mixture of **3a** (0.200 g, 0.298 mmol) and $Ph_2P(CH_2)_4PPh_2$ (0.115 g, 0.269 mmol) in CH_2Cl_2 (50 mL) was stirred for 3 h at room temperature. Activated charcoal was added to the solution, which was stirred for a further 0.5 h then filtered. The filtrate was concentrated (ca. 1–2 mL) and addition of pentane (100 mL) precipitated a white solid. The powder was collected by filtration, washed with diethyl ether and pentane, and dried. Yield 0.228 g, 77%; IR (CH_2Cl_2): $\tilde{\nu}$ = 2134 cm^{-1} (w) (C≡C); ^1H NMR (600 MHz, CD_2Cl_2, 25 °C): δ = 7.61–7.41 (m, 20H; Ph), 7.05 (m, 4H; C_6H_4), 6.95 (m, 4H; C_6H_4), 4.77 (s, 4H; OCH_2), 2.39 (m, 4H; CH_2), 1.72 (m, 4H; CH_2); ^{31}P NMR (160 MHz, CD_2Cl_2, 25 °C): δ = 38.75; ^{13}C NMR (150 MHz, CD_2Cl_2, 25 °C): δ = 154.0, 152.2 (both C_6H_4), 133.6 (d, ^2J(P,C) = 13 Hz; Ph), 132.2 (d, ^2J(P,C) = 143 Hz; C≡C), 131.9 (Ph), 130.5 (d, ^1J(P,C) = 54 Hz; Ph), 129.5 (d, ^3J(P,C) = 11 Hz; Ph), 119.8, 116.5 (both C_6H_4), 97.5 (d, ^3J(P,C) = 26 Hz; C≡C), 57.2 (OCH_2), 27.8 (d, ^1J(P,C) = 33 Hz; CH_2), 27.4 (br m; CH_2); elemental analysis calcd (%) for $C_{46}H_{40}Au_2P_2O_3$ (1096.7): C 50.38, H 3.68; found: C 50.90, H 3.83.

Simple ring 4b: This was prepared by the procedure described for **4a** from **3b** (0.200 g, 0.298 mmol) and $Ph_2P(CH_2)_4PPh_2$ (0.110 g, 0.269 mmol). The product was isolated as a white solid. Yield 0.215 g, 75%; IR (CH_2Cl_2): $\tilde{\nu}$ = 2135 cm^{-1} (w) (C≡C); ^1H NMR (600 MHz, CD_2Cl_2, 25 °C): δ = 7.64–7.41 (m, 20H; Ph), 7.35 (m, 4H; C_6H_4), 7.04 (m, 4H; C_6H_4), 4.78 (s, 4H; OCH_2), 2.34 (m, 4H; CH_2), 1.73 (m, 4H; CH_2); ^{31}P NMR (160 MHz, CD_2Cl_2, 25 °C): δ = 38.89; ^{13}C NMR (150 MHz, CD_2Cl_2, 25 °C): δ = 157.9 (C_6H_4), 133.6 (d, ^2J(P,C) = 13 Hz; Ph), 133.3 (C_6H_4), 132.1 (d, ^2J(P,C) = 133 Hz; C≡C), 131.9 (Ph), 130.6 (d, ^1J(P,C) = 52 Hz; Ph), 129.5 (d, ^3J(P,C) = 11 Hz; Ph), 127.7, 116.3 (both C_6H_4), 97.2 (C≡C), 57.1 (OCH_2), 27.9 (d, ^1J(P,C) = 35 Hz; CH_2P), 27.5 (br m; CH_2); elemental analysis calcd (%) for $C_{46}H_{40}Au_2P_2O_2S$ (1112.8): C 49.65, H 3.62; found: C 49.96, H 3.66.

Singly braided [2]catenane 4c: This was prepared by the procedure described for **4a** from **3c** (0.100 g, 0.150 mmol) and $Ph_2P(CH_2)_4PPh_2$ (0.057 g, 0.135 mmol). The product was isolated as a white solid. Yield 0.089 g, 61%; IR (CH_2Cl_2): $\tilde{\nu}$ = 2134 cm^{-1} (w) (C≡C); ^1H NMR (400 MHz, CD_2Cl_2, 25 °C): δ = 7.61–7.42 (m, 40H; Ph), 7.15 (m, 8H; C_6H_4), 6.98 (m, 8H; C_6H_4), 4.77 (s, 8H; OCH_2), 3.83 (s, 4H; CH_2), 2.32 (m, 8H; CH_2), 1.71 (m, 8H; CH_2); ^{31}P NMR (160 MHz, CD_2Cl_2, 25 °C): δ = 38.89; ^{13}C NMR (150 MHz, CD_2Cl_2, 25 °C): δ = 156.4, 134.4 (both C_6H_4), 133.6 (d, ^2J(P,C) = 13 Hz; Ph), 132.0 (d, ^2J(P,C) = 143 Hz; C≡C), 131.9 (Ph), 130.6 (d, ^1J(P,C) = 54 Hz; Ph), 129.7 (C_6H_4), 129.5 (d, ^3J(P,C) = 11 Hz; Ph), 115.3 (C_6H_4), 97.5 (d, ^3J(P,C) = 27 Hz; C≡C), 56.5 (OCH_2), 40.6 (CH_2), 28.0 (d, ^1J(P,C) = 34 Hz; CH_2P), 27.7 (dd, ^2J(P,C) = 20 Hz, ^3J(P,C) = 5 Hz; CH_2); elemental analysis calcd (%) for $C_{94}H_{84}Au_4P_4O_4$ (2189.5): C 51.57, H 3.87; found: C 51.70, H 3.88.

Singly braided [2]catenane 4d: This was prepared by the procedure described for **4a** from **3d** (0.115 g, 0.165 mmol) and $Ph_2P(CH_2)_4PPh_2$ (0.078 g, 0.183 mmol). The product was isolated as a white solid. Yield 0.125 g, 68%; IR (CH_2Cl_2): $\tilde{\nu}$ = 2132 cm^{-1} (w) (C≡C); ^1H NMR (300 MHz, CD_2Cl_2, 25 °C): δ = 7.64–7.42 (m, 40H; Ph), 7.20 (m, 8H; C_6H_4), 7.00 (m, 8H; C_6H_4), 4.76 (s, 8H; OCH_2), 2.35 (m, 8H; CH_2), 1.74 (m, 8H; CH_2), 1.64 (s, 12H; Me); ^{31}P NMR (120 MHz, CD_2Cl_2, 25 °C): δ = 38.73; ^{13}C NMR (150 MHz, CD_2Cl_2, 25 °C): δ = 156.6, 143.9 (both C_6H_4), 134.0 (d, ^2J(P,C) = 14 Hz; Ph), 132.5 (d, ^2J(P,C) = 143 Hz; C≡C), 132.3 (Ph), 131.1 (d, ^1J(P,C) = 53 Hz; Ph), 129.9 (d, ^3J(P,C) = 11 Hz; Ph), 128.2, 115.2 (both C_6H_4), 98.2 (d, ^3J(P,C) = 26 Hz; C≡C), 57.2 (OCH_2), 42.2 (CMe_2), 31.5 (Me), 28.5 (d, ^1J(P,C) = 34 Hz; CH_2), 28.2 (dd, ^2J(P,C) = 20 Hz, ^3J(P,C) = 6 Hz; CH_2); elemental analysis calcd (%) for $C_{98}H_{92}Au_4P_4O_4$ (2245.6): C 52.42, H 4.15; found: C 52.46, H 4.20.

Doubly braided [2]catenane 4e: This was prepared by the procedure described for **4a** from **3e** (0.100 g, 0.136 mmol) and $Ph_2P(CH_2)_4PPh_2$ (0.052 g, 0.122 mmol). The product was isolated as a white solid. Yield 0.103 g, 72%; IR (CH_2Cl_2): $\tilde{\nu}$ = 2134 cm^{-1} (w) (C≡C); ^1H NMR (600 MHz, CD_2Cl_2, 25 °C): δ = 7.61–7.43 (m, 80H; Ph), 7.23 (m, 16H; C_6H_4), 6.98 (m, 16H; C_6H_4), 4.76 (s, 16H; $2OCH_2$), 2.33 (m, 16H; CH_2), 2.22 (m, 16H; C_6H_{10}), 1.72 (m, 16H; CH_2), 1.51 (m, 24H; C_6H_{10}); ^{31}P NMR (160 MHz, CD_2Cl_2, 25 °C): δ = 38.75; ^{13}C NMR (150 MHz, CD_2Cl_2, 25 °C): δ = 155.7, 141.5 (both C_6H_4), 133.6 (d, ^2J(P,C) = 13 Hz; Ph), 132.0 (d, ^2J(P,C) = 143 Hz; C≡C), 131.9 (Ph), 130.6 (d, ^1J(P,C) = 53 Hz; Ph), 129.5 (d, ^3J(P,C) = 11 Hz; Ph), 128.1, 114.8 (both C_6H_4), 97.7 (d, ^3J(P,C) = 26 Hz; C≡C), 56.6 (OCH_2), 45.0 (C_6H_{10}), 37.7 (C_6H_{10}), 28.1 (d, ^1J(P,C) = 35 Hz; CH_2), 27.8 (br m; CH_2), 23.3 (C_6H_{10}); elemental analysis calcd (%) for $C_{208}H_{200}Au_8P_8O_8$ (4651.4): C 53.71, H 4.33; found: C 53.59, H 4.38.

X-ray structure determinations

Compound ***4a***: Crystals of $[\{\mu\text{-}O(C_6H_4OCH_2CCAu)_2\}\{\mu\text{-}[Ph_2P(CH_2)_4PPh_2]\}] \cdot 0.4\,CH_2Cl_2 \cdot 0.6\,Et_2O$ were grown from slow diffusion of diethyl ether into a solution of **4a** in dichloromethane. A colorless, trapezoidal plate was mounted on a glass fibre and data were collected at low temperature (150 K) by using a Nonius Kappa-CCD diffractometer with COLLECT (Nonius, 1998) software. The unit cell parameters were calculated and refined from the full data set. Crystal cell refinement and data reduction was carried out with the Nonius DENZO package. The data were scaled by using SCALEPACK (Nonius, 1998) and no other absorption corrections were applied. All crystal data and refinement parameters are listed in Table 7. The SHELXTL 5.1 (G. M. Sheldrick, Madison, W.I.) program package was used to solve the structure by direct methods, followed by successive difference Fourier transformations and refined with full-matrix least-squares procedures based on F^2. All non-hydrogen atoms were refined anisotropically. The hydrogen atoms were calculated geometrically, riding on their respective carbon atoms. The two solvent molecules occupied similar positions in space and thus the model consisted of two parts. 40% was isotropic CH_2Cl_2, and C–Cl (1.65 Å) and Cl–Cl (2.74 Å) were fixed. The remainder (60%) was isotropic diethyl ether, and two distances were also fixed C–C (1.54 Å), C–O (1.46 Å).

Compound ***4b***: Crystals of $[\{\mu\text{-}S(C_6H_4OCH_2CCAu)_2\}\{\mu\text{-}[Ph_2P(CH_2)_4PPh_2]\}] \cdot 0.5\,CH_2Cl_2 \cdot 0.5\,Et_2O \cdot 0.5\,Et_2O$ were grown from slow diffu-

Table 7. Crystal data and structure refinement for compounds **4a**–**e**.

	4a	**4b**	**4c**	**4d**	**4e**
formula	$C_{97.6}H_{93.6}Au_4Cl_{1.6}O_{7.2}P_4$	$C_{48.5}H_{40}Au_2Cl_1O_{2.5}P_2S_1$	$C_{97}H_{90}Au_4Cl_6O_4P_4$	$C_{50.25}H_{47.25}Au_2C_{l3.75}O_2P_2$	$C_{211}H_{220}Au_8Cl_6O_{15}P_8$
M_r	2350.19	1186.19	2444.14	1271.94	5032.06
crystal size [mm]	$0.38 \times 0.28 \times 0.10$	$0.31 \times 0.14 \times 0.14$	$0.23 \times 0.12 \times 0.06$	$0.49 \times 0.38 \times 0.05$	$0.68 \times 0.30 \times 0.04$
T [K]	150(2)	200(2)	200(2)	200(2)	293(2)
λ ($Mo_{K\alpha}$) [Å]	0.71073	0.71073	0.71073	0.71073	0.71073
crystal system	monoclinic	monoclinic	triclinic	triclinic	monoclinic
space group	$C2/c$	$C2/c$	$P\bar{1}$	$P\bar{1}$	$P2_1/n$
a [Å]	35.268(2)	35.8996(11)	11.2286(2)	15.7561(4)	27.1682(3)
b [Å]	13.1212(8)	13.1984(6)	16.9490(7)	16.1929(5)	27.9905(4)
c [Å]	24.5011(15)	26.7585(8)	25.5031(7)	21.2826(7)	31.9272(2)
α [°]	90	90	76.3620(10)	106.5450(10)	90
β [°]	130.187(2)	131.9430(10)	82.4150(10)	97.8420(10)	91.280(1)
γ [°]	90	90	80.8050(10)	102.6600(10)	90
V [Å^3]	8661.5(9)	9430.5(6)	4633.6(2)	4962.5(3)	24273.0(5)
Z	4	8	2	4	4
ρ_{calcd} [g cm^{-3}]	1.802	1.671	1.752	1.702	1.377
μ [mm^{-1}]	6.934	6.421	6.604	6.209	4.983
$F(000)$	4560	4576	2364	2466	9840
absorption correction	INTEGRATION	INTEGRATION	INTEGRATION	INTEGRATION	SADABS
transmission range	0.5439 – 0.1781	0.4667 – 0.2408	0.6927 – 0.3119	0.7424 – 0.1508	0.4928 – 0.2823
θ limits [°]	2.75/27.65	2.76/27.49	2.60/30.07	2.58/32.70	1.77/23.26
measured reflections	31776	26544	56922	70232	90406
unique reflections	9812 ($R_{int} = 0.085$)	10773 ($R_{int} = 0.085$)	26702 ($R_{int} = 0.0750$)	34852 ($R_{int} = 0.1120$)	33924 ($R_{int} = 0.1064$)
parameters	462	438	940	1103	1549
GOF on F^2	1.058	1.003	0.888	0.989	1.124
$R1$ [$I > 2\sigma(I)$]	0.1005	0.0543	0.0515	0.0957	0.1295
$wR2$ (on F^2, all data)	0.2780	0.1623	0.1248	0.2820	0.3032
$\Delta\rho_{min/max}$ [e Å^{-3}]	7.186/ – 4.393	2.375/ – 1.561	1.500/ – 2.765	4.0267 – 10.630	1.253/ – 2.412

sion of diethyl ether into a solution of **4b** in dichloromethane. A colorless block was mounted on a glass fibre. Data were collected at low temperature (200 K) and treated as above. All non-hydrogen atoms were refined anisotropically. The phenyl rings were refined as rigid hexagons. The hydrogen atoms were calculated geometrically, riding on their respective carbon atoms. In addition to the gold dimer, there were three sites of solvation. The methylene chloride was refined with a site occupation factor of 0.5. There were two half molecules of diethyl ether found on symmetry sites, and the C–C (1.54 Å) and C–O (1.45 Å) distances were fixed. All three molecules of solvation were modelled as isotropic atoms. No hydrogens were incorporated into the solvent models. The largest residual electron density peak (2.375 e A^{-3}) was associated with one of the solvent molecules.

Compound ***4c***: Crystals of $[\{\mu\text{-}H_2C(C_6H_4OCH_2CCAu)_2\}\{\mu\text{-}[Ph_2P(CH_2)_4PPh_2]\}]_2 \cdot 3\,CH_2Cl_2$ were grown from slow diffusion of diethyl ether into a solution of **4c** in dichloromethane. A colorless, rectangular plate was mounted on a glass fibre. Data were collected at room temperature (295 K) and treated as above. All non-hydrogen atoms were refined anisotropically. The hydrogen atoms were calculated geometrically, riding on their respective carbon atoms. Of the three solvent molecules two were constrained to have the same geometry as the first.

Compound ***4d***: Crystals of $[\{\mu\text{-}Me_2C(C_6H_4OCH_2CCAu)_2\}\{\mu\text{-}[Ph_2P(CH_2)_4PPh_2]\}]_2 \cdot 2.5\,CDCl_3$ were grown from slow diffusion of diethyl ether into a solution of **4d** in deutero-chloroform. A colorless plate was mounted on a glass fibre. Data were collected at room temperature (295 K) and treated as above. All non-hydrogen atoms were refined with anisotropic thermal parameters. The hydrogen atoms were calculated geometrically and were either riding, or in the case of methyl groups, riding as rigid groups on their respective carbon atoms. The solvent molecules were refined anisotropically.

Compound ***4e***: Crystals of $[\{\mu\text{-}H_{10}C_6(C_6H_4OCH_2CCAu)_2\}_2\{\mu\text{-}[Ph_2P(CH_2)_4PPh_2]\}]_2 \cdot 3\,CH_2Cl_2$ were grown from slow diffusion of diethyl ether into a solution of **4e** in dichloromethane. A long thin plate was mounted inside a capillary tube and flame sealed. Data were collected at room temperature (293 K) on a Bruker SMART CCD diffractometer with a $Mo_{K\alpha}$ sealed tube. The collected frames were integrated by using the preliminary cell-orientation matrix. The software used was SMART, for collecting frames of data, indexing reflection and determination of lattice parameters; SAINT, for integration of intensity of reflections and scaling; SADABS, for absorption correction; and SHELXTL, for space group and structure determination, least-squares refinements on F^2, graphics, and structure reporting. The crystal was weakly diffracting. Anisotropic thermal parameters were refined for all the non-carbon atoms in the main structure except for all the phenyl rings of dppb units and one cyclohexyl ring (C(82) – C(87)). The carbon atoms of this cyclohexyl ring and in many other phenyl rings showed high isotropic thermal parameters. The C–C bond lengths in the cyclohexyl ring were fixed at 1.540 Å and C···C distances were constrained to be equal. A common isotropic thermal parameter was refined for these carbon atoms. Ideal hexagon geometry was imposed for all the phenyl rings in dppb units, except the rings with suffixes a, b, c, i, j, and l. Individual isotropic temperature factors were refined for these carbon atoms. The electron densities in the Fourier difference maps revealed the presence of disordered CH_2Cl_2 solvent in seven places in the asymmetric unit and totaled three molecules. Further unrelated peaks in the difference Fourier were tentatively assigned to the oxygen atoms of the seven water molecules in total. Of the 23 fragments, five were assigned occupancies of 0.5 and the rest 0.25. No hydrogen atoms were included for the solvent atoms. Final agreement factors reflect the poor quality data due to poor quality of the crystal. However, all heavy atoms were clearly identified, and the connectivity of the organometallic rings is proved beyond any doubt.

Crystallographic data (excluding structure factors) for the structures reported in this paper have been deposited with the Cambridge Crystallographic Data Centre as supplementary publication no. CCDC 158705 (**4a**), CCDC 158706 (**4b**), CCDC 158704 (**4c**), CCDC 120857 (**4d**) and CCDC 145603 (**4e**). Copies of the data can be obtained free of charge on application to CCDC, 12 Union Road, Cambridge CB2 1EZ, UK (fax: (+44) 1223-336-033; e-mail: deposit@ccdc.cam.ac.uk).

Acknowledgements

We thank Dr. C. Kirby (UWO) for assistance with NMR experiments and the National Science and Engineering Research Council (Canada) for financial support. Funding from the National University of Singapore for the purchase of a Bruker AXS CCD diffractometer is also gratefully acknowledged.

  0947-6539/01/0716-3582 $ 17.50+.50/0

[1] a) D. M. Walba, *Tetrahedron* **1985**, *41*, 3161–3212; b) H. Dodzuik, K. S. Nowinski, *Tetrahedron* **1998**, *54*, 2917–2930; c) G. A. Breault, C. A. Hunter, P. C. Mayers, *Tetrahedron* **1999**, *55*, 5265–5293; d) A. Sobanski, R. Schmieder, F. Vögtle, *Chem. Unserer Zeit* **2000**, *34*, 160–169.

[2] a) E. Wasserman, *J. Am. Chem. Soc.* **1960**, *82*, 4433–4434; b) H. L. Frisch, E. Wasserman, *J. Am. Chem. Soc.* **1961**, *83*, 3789–3795.

[3] a) J.-P. Sauvage, C. O. Dietrich-Buchecker, J.-C. Chambron, in *Comprehensive Supramolecular Chemistry, Vol. 2* (Eds.: J.-M. Lehn, J. L. Atwood, J. E. D. Davies, D. D. McNicol, F. Vögtle, J.-P. Sauvage, M. W. Hosseini) Pergamon, Oxford, **1995**, Chapter 2, pp. 43–83; b) J.-C. Chambron, C. O. Dietrich-Buchecker, V. Heitz, J.-F. Nierengarten, J.-P. Sauvage, C. Pascard, J. Guilhem, *Pure Appl. Chem.* **1995**, *67*, 233–240; c) R. Hoss, F. Vögtle, *Angew. Chem.* **1994**, *106*, 389–398; *Angew. Chem. Int. Ed. Engl.* **1994**, *33*, 375–384; d) M. Fujita, *Acc. Chem. Res.* **1999**, *32*, 53–61.

[4] a) O. Safarowsky, M. Nieger, R. Fröhlich, F. Vögtle, *Angew. Chem.* **2000**, *112*, 1699–1701; *Angew. Chem. Int. Ed.* **2000**, *39*, 1616–1618; b) C. Seel, F. Vögtle, *Chem. Eur. J.* **2000**, *6*, 21–24; c) T. J. Kidd, D. A. Leigh, A. J. Wilson, *J. Am. Chem. Soc.* **1999**, *121*, 1599–1600; d) K. N. Houk, S. Menzer, S. P. Newton, F. M. Raymo, J. F. Stoddart, D. J. Williams, *J. Am. Chem. Soc.* **1999**, *121*, 1479–1487; e) D. G. Hamilton, J. E. Davies, L. Prodi, J. K. M. Sanders, *Chem. Eur. J.* **1998**, *4*, 608–620; f) F. Vögtle, T. Dünnwald, T. Schmidt, *Acc. Chem. Res.* **1996**, *29*, 451–460.

[5] a) G. Schill, *Catenanes, Rotaxanes and Knots*, Academic Press, New York, **1971**; b) J.-P. Sauvage, C. O. Dietrich-Buchecker, in *Molecular Catenanes, Rotaxanes and Knots* (Eds.: J.-P. Sauvage, C. O. Dietrich-Buchecker) Wiley-VCH, Weinheim, **1999**; c) F. M. Raymo, J. F. Stoddart, *Chem. Rev.* **1999**, *99*, 1643–1663; d) D. B. Amabilino, J. F. Stoddart, *Chem. Rev.* **1995**, *95*, 2725–2828.

[6] a) M. Consuelo Jimenez, C. Dietrich-Buchecker, J.-P. Sauvage, A. De Cian, *Angew. Chem.* **2000**, *112*, 1351–1354; *Angew. Chem. Int. Ed.* **2000**, *39*, 1295–1298; b) S. Leininger, B. Olenyuk, P. J. Stang, *Chem. Rev.* **2000**, *100*, 853–908; c) M. Fujita, N. Fujita, K. Ogura, K. Yamaguchi, *Nature* **1999**, *400*, 52–55; d) S.-G. Roh, K.-M. Park, G.-J. Park, S. Sakamoto, K. Yamaguchi, K. Kim, *Angew. Chem.* **1999**, 111, 672–675; *Angew. Chem. Int. Ed.* **1999**, *38*, 638–640; e) S. R. Batten, R. Robson, *Angew. Chem.* **1998**, 110, 1558–1595; *Angew. Chem. Int. Ed.* **1998**, *37*, 1460–1494.

[7] a) V. Balzani, A. Credi, F. M. Raymo, J. F. Stoddart, *Angew. Chem.* **2000**, *112*, 3484–3530; *Angew. Chem. Int. Ed.* **2000**, *39*, 3348–3391; b) C. P. Collier, E. W. Wong, M. Belohradsky, F. M. Raymo, J. F. Stoddart, P. J. Kuekes, R. S. Williams, J. R. Heath, *Science* **1999**, *285*, 391–394.

[8] a) C. O. Dietrich-Buchecker, J.-P. Sauvage, *Chem. Commun.* **1999**, 615–616; b) F. Ibukuro, M. Fujita, K. Yamaguchi, J.-P. Sauvage, *J. Am. Chem. Soc.* **1999**, *121*, 11014–11015.

[9] a) W. J. Hunks, M. C. Jennings, R. J. Puddephatt, *Inorg. Chem.* **1999**, *38*, 5930–5932; b) R. J. Puddephatt, *Chem. Commun.* **1998**, 1055–1062; c) M. J. Irwin, J. J. Vittal, R. J. Puddephatt, *Organometallics* **1997**, *16*, 3541–3547; d) M. J. Irwin, L. Manojlovic Muir, K. W. Muir, R. J. Puddephatt, D. S. Yufit, *Chem. Commun.* **1997**, 219–220.

[10] A. Grohmann, H. Schmidbaur, in *Comprehensive Organometallics II, Vol. 3* (Eds.: E. Abel, F. G. A. Stone, G. Wilkinson) Elsevier, Oxford, **1995**, pp. 1–5.

[11] a) H. Schmidbaur, A. Grohmann, M. E. Olmos, in *Gold: Progress in Chemistry, Biochemistry and Technology* (Ed.: H. Schmidbaur), Wiley, Chichester, **1999**, Chapter 18; b) P. Pyykkö, *Chem. Rev.* **1997**, *97*, 597–636.

[12] C. P. McArdle, M. J. Irwin, M. C. Jennings, R. J. Puddephatt, *Angew. Chem.* **1999**, *111*, 3571–3573; *Angew. Chem. Int. Ed.* **1999**, *38*, 3376–3378.

[13] C. P. McArdle, J. J. Vittal, R. J. Puddephatt, *Angew. Chem.* **2000**, *112*, 3977–3980; *Angew. Chem. Int. Ed.* **2000**, *39*, 3819–3822.

[14] a) M. J. Irwin, J. J. Vittal, G. P. A. Yap, R. J. Puddephatt, *J. Am. Chem. Soc.* **1996**, *118*, 13101–13102; b) M. J. Irwin, G. C. Jia, N. C. Payne, R. J. Puddephatt, *Organometallics* **1996**, *15*, 51–57.

[15] G. E. Coates, C. Parkin, *J. Chem. Soc.* **1962**, 3220–3226.

[16] D. M. P. Mingos, J. Yau, S. Menzer, D. J. Williams, *Angew. Chem.* **1995**, *107*, 2045–2047; *Angew. Chem. Int. Ed. Engl.* **1995**, *34*, 1894–1895.

[17] K. Higasi, S. Uyeo, *Bull. Chem. Soc. Japan* **1939**, *14*, 87–101.

[18] a) I. Dance, M, Scudder, *Chem. Eur. J.* **1996**, *2*, 481–486; b) C. A. Hunter, *Chem. Soc. Rev.* **1994**, *23*, 101–109; c) C. A. Hunter, J. K. M. Sanders, *J. Am. Chem. Soc.* **1990**, *112*, 5525–5534.

[19] K. von Deuten, G. Klar, *Cryst. Struct. Commun.* **1981**, *10*, 231–238.

[20] a) Q. Zhang, D. G. Hamilton, N. Feeder, S. J. Teat, J. M. Goodman, J. K. M. Sanders, *New J. Chem.* **1999**, *23*, 897–903; b) B. Cabezon, J. Cao, F. M. Raymo, J. F. Stoddart, A. J. P. White, D. J. Williams, *Angew. Chem.* **2000**, *112*, 152–155; *Angew. Chem. Int. Ed.* **2000**, *39*, 148–151; c) C. A. Hunter, *J. Am. Chem. Soc.* **1992**, *114*, 5303–5311

[21] CSD Version 5.19 (April **2000**), CCDC ConQuest Version 1.0, Copyright CCDC **2000**.

[22] M. S. Deleuze, D. A. Leigh, F. Zerbetto, *J. Am. Chem. Soc.* **1999**, *121*, 2364–2379.

[23] a) J.-F. Nierengarten, C. O. Dietrich-Buchecker, J.-P. Sauvage, *J. Am. Chem. Soc.* **1994**, *116*, 375–376; b) J.-F. Nierengarten, C. O. Dietrich-Buchecker, J.-P. Sauvage, *New J. Chem.* **1996**, *20*, 685–693.

[24] A. Tamaki, J. K. Kochi, *J. Organomet. Chem.* **1974**, *64*, 411–425.

Received: April 2, 2001 [F3173]